Medium-range structural order and fractal annealing kinetics of radiolytic atomic hydrogen in high-purity silica

T. E. Tsai,* D. L. Griscom, and E. J. Friebele
Naval Research Laboratory, Washington, D.C. 20375-5000
(Received 20 March 1989)

Thermal annealing of radiation-induced atomic hydrogen in OH-containing high-purity silicas was studied by electron-spin resonance (ESR) in the temperature range 75–185 K. Both 100-keV x rays and 6.4-eV excimer-laser light were used to generate the H^0. In general, the isothermal anneal curves consisted of two components, one approaching a t^{-1} law at long times, and the other taking on a $t^{-2/3}$ dependence at still longer times. All data are interpreted in terms of bimolecular kinetics, assuming dimerization of the radiolytic H^0 and/or its reaction with other paramagnetic species in the glass. The t^{-1} behavior follows directly from classical second-order kinetics. Fractal kinetics is used to explain the long-time fractional–power-law annealing behaviors. Diffusion in medium-range structural channels in silica is suggested as the origin of the observed fractal kinetics. Data consistent with this proposal are presented.

I. INTRODUCTION

The short-range structural order in amorphous materials is well established from diffraction studies.[1] Experimental data supporting the existence of medium-range structural order in chalcogenide glasses were reported recently.[2–5] Brukner[6] has summarized a variety of indirect evidence for changes in the medium-range order of silica as a function of heat treatment. Konnert *et al.*[7] interpreted their x-ray-diffraction data for silica in terms of a tridymite-like intermediate-range structure ≈ 20 Å (tridymite is one of the crystalline polymorphs of SiO_2). More recently, Galeener and Wright[8] have reviewed many models for the intermediate-range order of amorphous SiO_2 against a background of the available diffraction and Raman-spectroscopic data.

In the case of oxides grown on Si single-crystal surfaces, evidence of medium-range order was obtained from a variety of techniques, including x-ray-photoelectron-spectroscopy (XPS) measurements[9] and reflection high-energy electron-diffraction (RHEED) measurements.[10] It has been suggested that the medium-range structural order in silica produced by thermal oxidation of silicon in dry O_2 might include oriented structural channels.[11] For reactions in such channels, fractal-like kinetics is expected at long times,[12] e.g., third-order reaction kinetics is anticipated for bimolecular reaction in well-oriented one-dimensional channels.[12] Experimentally, it appears that radiation-induced atomic hydrogen in thermally grown silica reacts with states at the SiO_2/Si interface to form electrically active interface defects according to third-order kinetics.[13]

Atomic hydrogen (H^0) is perhaps the ideal atom for probing the medium-range order in amorphous solids, especially in silica. Not only can its time-dependent behavior be studied by ESR, but, with a diameter of about 1 Å, H^0 can be used to probe structural order down to several angstroms. Atomic hydrogen can be produced in hydroxyl-containing silica by radiolysis of $\equiv$Si—OH groups:

$$\equiv\text{Si—OH} \xrightarrow{h\nu} \equiv\text{Si—O}^{\cdot} + \text{H}^0 \ .$$

We have reported recently[14] that the thermal annealing of radiation-induced atomic hydrogen in high-purity silica containing a high concentration of hydroxyl ions is dispersive and requires the use of fractal kinetics to describe its annealing behavior at long times. Structural channels similar to those proposed to exist in thermally grown amorphous SiO_2 were suggested as the root of the observed fractal annealing kinetics in bulk fused silica.

In this paper we describe our experiments in more detail and provide further data consistent with the existence of these structural channels.

II. EXPERIMENT

High-purity type-III synthetic silicas (Suprasil 1 and 2 manufactured by Heraeus Amersil) produced by flame hydrolysis of $SiCl_4$ and containing about 1200 ppm OH were used for this study. Suprasil 1 is of higher optical quality and is made from Suprasil 2 by high-temperature thermal annealing to remove optical bubbles. Samples comprising rods of diameter 4 mm and length ≈ 40 mm were irradiated at 77 K with either 100-keV x rays or 6.4-eV photons from an ArF excimer laser (Lambda Physiks, Inc.). *X*-band ESR spectra ($\nu \approx 9.4$ GHz) were obtained with a Bruker ER 200D-SRC spectrometer employing 100-kHz field modulation for first-harmonic detection or 50-kHz modulation when recording in the second-harmonic mode. The spectrum of atomic hydrogen is manifested as a well-known hyperfine doublet with splitting ≈ 50.5 mT centered on $g = 2.0$. Isothermal (75–185 K) and isochronal (100–160 K) annealing experiments (5 min at temperature) were carried out *in situ* with temperature regulation (precision ± 0.5 K) by means of a nitrogen flowthrough device.

 ©1989 The American Physical Society

III. THEORY

In classical gas-phase reactions the kinetics of reactions $A+A\rightarrow$(products) or $A+B\rightarrow$(products) are described by solutions of

$$d[A]/dt=-K[A]^2 \tag{1}$$

or

$$d[A]/dt=-K[A][B]\ , \tag{2}$$

respectively, where K is a time-independent rate constant. The solution of Eq. (1) approaches $[A]/[A]_0\propto t^{-1}$ at long time t.

As recently reviewed by Kopelman,[12] quite different results are obtained for reactions occurring in fractal dimensions d_f which are lower than the dimension d of the Euclidian space in which the fractal is embedded. In such cases, the kinetic laws can be obtained as solutions of Eqs. (1) or (2) where K is replaced by kt^{-h} $(0<h\leq 1)$. The apparent time dependence of the rate "constant" derives from consideration of the recurrence probability P of a random walker; that is, the probability that a random walker will return to its starting point after a period of time t:

$$P\propto\begin{cases} t^{-d_s/2}, & d_s\leq 2 \\ t^{-1}, & d_s>2\ . \end{cases} \tag{3}$$

In Eq. (3), d_s is the "spectral dimension," which differs in general from the fractal dimension,[12] but always satisfies the inequality $d>d_f>d_s$. As a consequence of Eq. (3), chemical reactants moving on a fractal of spectral dimension less than 2 have a higher probability of returning to their starting points (and hence failing to react with their neighbors) than do reactants in dimensions greater than 2. In the case of $A+B$ reactions, actual *segregation of reactants* takes place and is the physical origin of the apparent time-dependent rate constant $\propto t^{-h}$, where the exponent h is given by[12] $h=1-d_s/2$. Kopelman[12] notes that for the whole class of random fractals (including the percolation cluster), in all embedded Euclidean dimensions (two, three, or higher), d_s is always $\approx\frac{4}{3}$. Thus, $h\approx\frac{1}{3}$ for $A+A$ reactions on random fractals.

It is customary[15–20] and convenient to express the time-dependent rate coefficient in the form

$$K(t)=kft^{f-1}\ , \tag{4}$$

where for classical reactions $f=1$. The solution of Eq. (1) is then

$$[A]/[A]_0=1/(1+k[A]_0t^f)\ . \tag{5}$$

In this notation, $f=1-h=d_s/2$. Therefore, for the class of random fractals $f\approx\frac{2}{3}$, resulting in a long-time dependence of $[A]\propto t^{-2/3}$.

IV. RESULTS AND DISCUSSION

A. Temperature dependence of the rate coefficients

Griscom[21] presented evidence and arguments that much of the atomic hydrogen produced by low-temperature irradiation of high-OH silicas must anneal by dimerization, $H^0+H^0\rightarrow H_2$. Accordingly, initial attempts were made to fit the isothermal anneal data of the present experiment using Eq. (5) with the exponent f as a free parameter. The apparent temperature dependence of f derived in this way is illustrated in Fig. 1(a). Here, f is noted to peak near 105 K and to increase again above $\approx$130 K. However, this analysis is clearly unsatisfactory, since f exceeds its classical value of 1 over much of the temperature range.

An important factor neglected in the modeling of Fig. 1(a) is that some of the radiolytic H^0 has been shown[21] to react with other defects in the glass in the temperature range 100–130 K. Typical reactions occur with oxygen-associated hole centers ($H^0+\equiv Si—O^{\cdot}\rightarrow \equiv SiOH$) and, in some cases, with dissolved CO molecules (H^0+CO

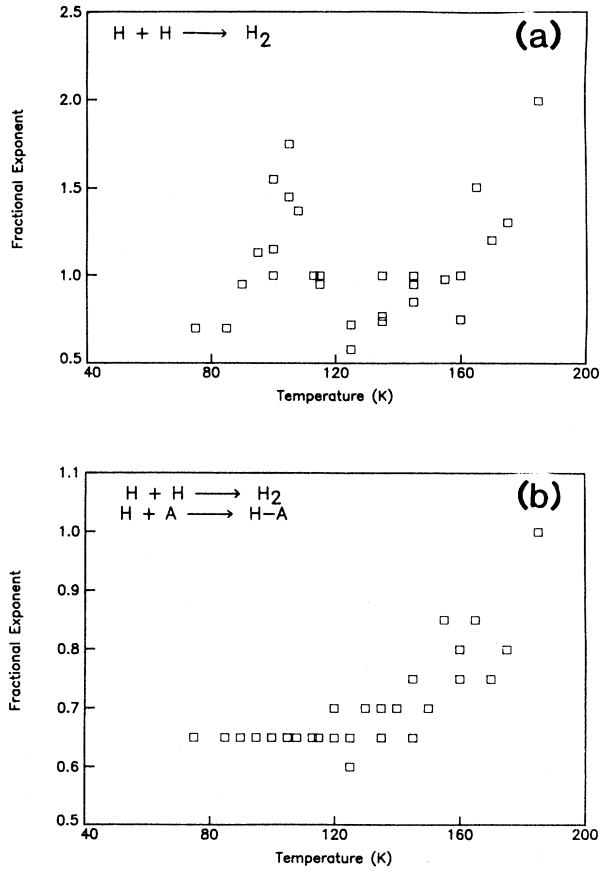

FIG. 1. Temperature dependence of fractional exponent f obtained from fits to our long-time isothermal anneal data for radiolytic atomic hydrogen in silica using (a) Eq. (5) and (b) Eq. (7).

$\rightarrow$HCO).[22] Therefore, the isothermal anneal data were reanalyzed by fitting to the solution of

$$d[\mathrm{H}]/dt = -ft^{f-1}(k_b[\mathrm{H}]^2 + k_a[\mathrm{H}][A]) , \quad (6)$$

where $[A]$ represents the sum of the concentrations of the other reactants (which may be OHC's, CO, etc.) and k_a and k_b are rate coefficients related to the diffusivity of hydrogen in silica. Since the various side reactions have been shown[21] to be typically far from completion at temperatures below ≈ 200 K, the approximation was made that $[A] \approx$ const in deriving the following solution for Eq. (6):

$$[\mathrm{H}]/[\mathrm{H}]_0 = 1/\{(1+F)\exp(k_a[A]t^f) - F\} . \quad (7)$$

In Eq. (7),

$$F = k_b[\mathrm{H}]_0/k_a[A] \quad (8)$$

is the ratio of the initial dimerization rate to the initial side-reaction rate, and $[\mathrm{H}]_0$ is the initial concentration of atomic hydrogen. (When $k_a[A] \rightarrow 0$, i.e., in the case that the side reactions are insignificant, Eq. (7) reduces to Eq. (5).)

The temperature dependence of f determined by fitting our isothermal anneal data with Eq. (7) is shown in Fig. 1(b).[23] For temperatures below ≈ 145 K, f is found to be 0.65 ± 0.05, independent of temperature, while, above 145 K, f increases with temperature and reaches the classical value of 1 at 185 K.[14]

B. Detailed fits of the isothermal anneal curves

Figure 2 shows typical isothermal annealing data at 135 K for atomic hydrogen induced in Suprasil 2 by a 10 Mrad x-ray exposure at 77 K. Two kinds of annealing kinetics are clearly occurring at the same time. The curve through the data points comprises the sum of the two components, corresponding to classical ($f = 1$) and fractal ($f = 0.65$) bimolecular kinetics, as indicated in the figure.

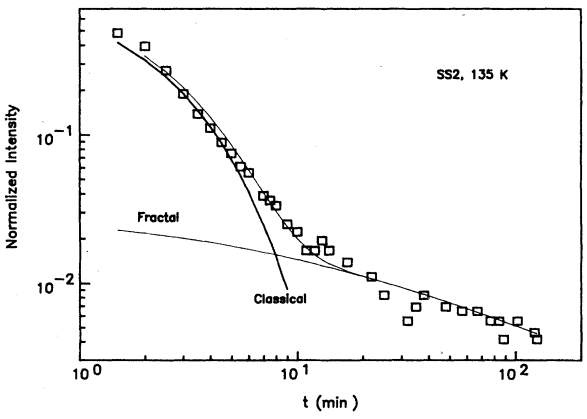

FIG. 2. Isothermal annealing of atomic hydrogen at 135 K in Suprasil 2 irradiated with 100-keV x rays to a dose of 10 Mrad at 77 K. The fitted curve is the sum of the two illustrated components, representing classical ($f = 1$) and fractal ($f < 1$) solutions of Eq. (6).

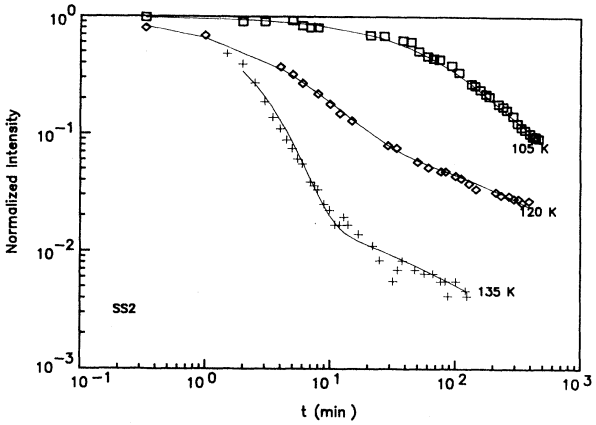

FIG. 3. Isothermal annealing of atomic hydrogen at various temperatures in Suprasil 2 irradiated with 100-keV x rays to a dose of 10 Mrad at 77 K. Fitted curves are linear combinations of classical ($f = 1$) and fractal ($f < 1$) solutions of Eq. (6).

Figure 3 shows the isothermal annealing of atomic hydrogen at various temperatures in Suprasil 2 irradiated with 10 Mrad of 100-keV x rays at 77 K. (The samples were kept in liquid nitrogen overnight before the ESR measurements were carried out.) The solid lines are the fitted curves, each assuming the two kinds of kinetics. The parameters used in the fits are shown in Table I.[24] Inspection of the table shows that the fraction of atomic hydrogen which decays classically increases with increasing temperature. For temperatures below about 90 K, fractal kinetics can be used to fit the annealing curves without involving classical kinetics (data not shown).

Figure 4 shows the temperature dependence of the bi-

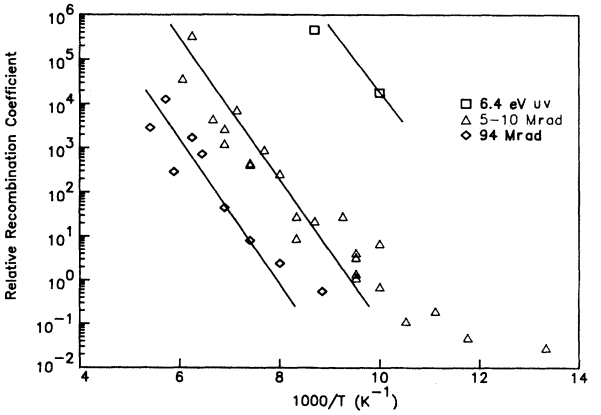

FIG. 4. Temperature dependence of the bimolecular reaction coefficient k_b of atomic hydrogen undergoing fractal anneal kinetics in Suprasil 2. Each point represents a separate isothermal anneal curve whose *long-time* behavior has been fitted to Eq. (7). Solid lines are linear regression fits of data for temperatures above 120 K.

TABLE I. Parameters describing the annealing behavior of atomic hydrogen in x-irradiated Suprasil 2 obtained from fits of the ESR-amplitude data to a linear combination of classical ($F_c = ([H]/[H]_0)_{f=1}$) and fractal ($F_f = ([H]/[H]_0)_{f=0.65}$) kinetics: $WF_c + (1-W)F_f$, where the functional form of $[H]/[H]_0$ is given by Eq. (7).

Temp. (K)	W	Rate coefficients: Classical kinetics $k_b[H]_0$	Classical kinetics $k_a[A]$	Fractal kinetics $k_b[H]_0$	Fractal kinetics $k_a[A]$
105	0.60	0.0105	0.0075	0.042	0.001[a]
120	0.89	0.09[a]	0.18	0.0383	0.001[a]
135	0.95	0.09[a]	0.5	0.153	0.001[a]

[a]The curve-fitting procedure was not sufficiently sensitive to determine the temperature dependence of these parameters. The values listed are those used in the fits which determined the other parameters; see Ref. 24.

molecular reaction coefficients (k_b) of the portion of the hydrogen undergoing fractal kinetics (i.e., the long-time annealing portion of the isothermal annealing curves), obtained from curve fitting using Eq. (7). For temperatures below about 120 K [$(1000\ \text{K})/T \gtrsim 8.33$], the bimolecular reaction coefficient k_b is almost independent of temperature. Above 120 K the activation energies for motion of the atomic hydrogen, calculated from the slopes of a linear regression fit of the data (neglecting the temperature-independent portions of the curves), are 0.21, 0.23±0.02, and 0.24±0.04 eV, respectively, for irradiation with 6.4-eV uv light, 3–10-Mrad x-rays, and 94-Mrad x rays. These values are identical within experimental error, independent of the irradiation source and dose, and are presumably more accurate than previous estimates (e.g., Ref. 13) made without the benefit of an Arrhenius plot.

C. Influence of manufacturing process

Since Suprasil 1 is made from Suprasil 2 by high-temperature heat treatment, the effects of such treatment can be studied by comparing these two samples. Figure 5 shows the isothermal annealing of atomic hydrogen at 135 K in Suprasil 1 and 2 irradiated with 10 Mrad of 100-keV x rays at 77 K and left overnight at 77 K. The decay of atomic hydrogen in Suprasil 2 is faster than in Suprasil 1. Corresponding behavior is also observed in the isochronal annealing shown in Fig. 6.

Using the two kinds of kinetics in the curve fitting as discussed above, we obtain from Fig. 5 the fractions of atomic hydrogen behaving according to classical kinetics of 0.9 and 0.7, respectively, in Suprasil 2 and in Suprasil 1. We note from Table I that (above 105 K) the classical components of the anneal curves are primarily associated with side reactions of H^0 with other reactants. Since HCO (the product of the reaction of H^0 with CO) is hardly observed in Suprasil 1, the decrease in the fraction of atomic hydrogen undergoing classical kinetics in Suprasil 1 is possibly related to the reduced HCO production, other things being equal. We point out that the OH content of Suprasil 1 is the same as that of the Suprasil 2 from which it is prepared. Since hydrogen should out-gas faster during heat treatment than the larger CO molecule, it seems unlikely that all of the CO has been removed from Suprasil 1. We therefore suggest that the portion of atomic hydrogen undergoing classical annealing kinetics is due to a subset of hydrogens that are paired up with their neighboring reactants and that the occurrence of H-CO pairs may be a characteristic of Suprasil 2. The decay of the paired reactants should be independent of the overall fractal dimension of the material in which they reside (and hence obey classical reaction kinetics).

As Table I shows, the fraction W of atomic hydrogen undergoing classical kinetics, which dominates their initial decay, increases with increasing temperature. This is expected since two reactants which may be paired but cannot react due to an energy barrier at lower temperatures can react at higher temperatures.

D. Medium-range structural order—Structural channels

Figures 5 and 6 show that the decay of atomic hydrogen in Suprasil 1 is slower than in Suprasil 2. At the

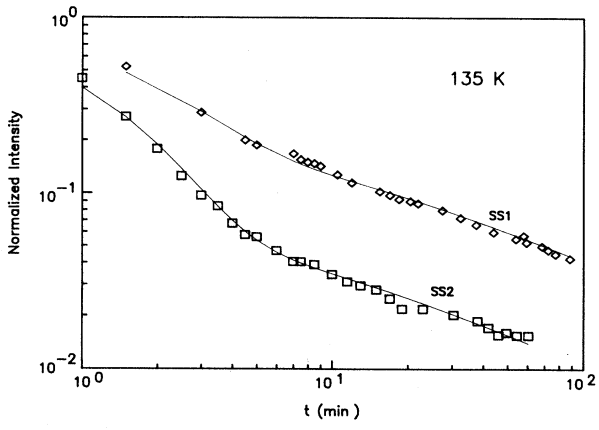

FIG. 5. Isothermal annealing of atomic hydrogen atoms at 135 K in Suprasil 2 and Suprasil 1 irradiated with 100-keV x rays at 77 K. Fitted curves are linear combinations of classical ($f=1$) and fractal ($f<1$) solutions of Eq. (6). The absolute concentrations of atomic hydrogen in Suprasil 2 and Suprasil 1 are 2.4×10^{16} and 8×10^{15} spins/g, respectively.

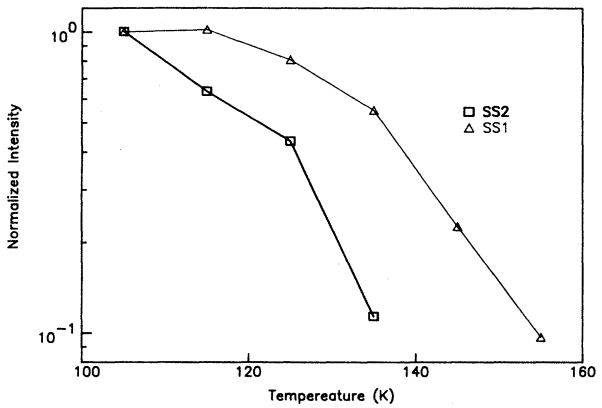

FIG. 6. Isochronal annealing of atomic hydrogen in Suprasil 2 and Suprasil 1 induced by 100-keV x rays at 77 K. The absolute concentrations of atomic hydrogen in Suprasil 2 and Suprasil 1 are 2.1×10^{13} and 3.9×10^{13} spins/g, respectively.

same time, HCO is hardly observed in Suprasil 1, but can be observed readily in Suprasil 2 after a brief postirradiation thermal anneal near 300 K (see Ref. 22). This observation suggests that the majority of the atomic hydrogen atoms induced in Suprasil 1 are at locations which are separated by high potential barriers from the interstitial CO presumed to be still present (see Sec. IV C). In the case of Suprasil 2, the atomic hydrogen formed is not separated from CO and hence HCO can form readily. It is then reasonable to suggest that the hydrogen atoms induced in Suprasil 1 are located inside structural channels (medium-range structure order of silica) (Ref. 11) which are too small to accommodate CO (bond length 1.5 Å).[25] These structural channels might also be the preordered regions proposed by Bruckner[6] in order to explain the complex volume behavior of vitreous silica annealed to various temperatures.

According to the discussion above, our experimental results can be understood in terms of a higher degree of medium-range order in Suprasil 1 relative to Suprasil 2. Since Suprasil 1 is the same material as Suprasil 2, except for high-temperature thermal treatment to anneal out optical bubbles, it is then suggested that the degree of medium-range order (that is, the lengths, volumes, and/or interconnectivity of structural channels) of silica increases with high-temperature thermal annealing. Analogous changes in the medium-range structural order after thermal annealing have also been reported in metallic glass.[26] In fact, positron-annihilation studies of the effects of heat treatment on silica glasses recently demonstrated[27] systematic increases in the degree of structural order with heat treatments in the range 900–1300 °C. In Ref. 21, changes in the isochronal anneal curves of radiolytic H^0 equivalent to the difference between Suprasil 1 and 2 in Fig. 6 were achieved by annealing a sample similar to present-day Suprasil 2 to 1100 °C overnight. Therefore, the degree of medium-range structural order in silica appears to increase with high-temperature heat treatment, leading to a higher fraction of atomic hydrogen undergoing fractal annealing kinetics in Suprasil 1 than in Suprasil 2.

E. The effect of irradiation type on the diffusivity of atomic hydrogen

Figure 4 shows that the activation energy for diffusion of atomic hydrogen for temperatures above ≈120 K is ≈0.24 eV, irrespective of the source of irradiation and irradiation dose (an increase in the average activation energy with increasing irradiation dose was observed in the linear regression fits, but the variations are within the error bars of the fits). The data clearly show that the effect of irradiation dose and sources on the diffusion of atomic hydrogen in silica is manifested not in the activation energy, but rather in the diffusion preexponential factor (the prefactors for irradiations with uv, 3–10-Mrad x rays and 94-Mrad x rays are 10, 1×10^{-2}, and 8×10^{-4} cm^2/s, respectively). This outcome is consistent with the report of Boesch and Moynihan[28] that the distribution of electrical relaxation times obtained from the temperature dependence of relaxation spectra of silicate glasses arises primarily from the distribution in the preexponential factors containing attempt frequency, entropy, and structure-related factors, rather than in activation enthalpy.

The value of 0.24 eV for the activation energy for the diffusion of atomic hydrogen in silica reported here is greater than the values of about 0.1 eV (Ref. 29) to 0.2 eV (Ref. 30) reported in sulfuric acid glasses, but is smaller than the values of 0.4 eV reported in nickel[31] and 0.9–1.0 eV in amorphous silicon.[32] The activation energy measured here is consistent with these results: Since the matrix of sulfuric glasses is less rigid than silica, a higher activation energy is expected to be observed in silica. On the other hand, since the structure of silica is more open than those of nickel or amorphous silicon, a lower activation energy is anticipated in silica.

For temperatures below about 120 K, bimolecular reaction coefficients tend to become independent of temperature (Fig. 4). This suggests that at lower temperatures the diffusion of atomic hydrogen involves quantum-mechanical tunneling rather than thermally assisted hopping.

The activation energy for the portion of the hydrogen subject to classical kinetics calculated from k_a in Table I is about 0.2 eV, which is virtually identical to the activation energy of 0.24 eV determined from Fig. 4 for hydrogen diffusion in fractal dimensions. This agreement is not surprising: Since the activation energy in classical kinetics is the energy barrier that must be surmounted for atomic hydrogen to react with its immediate neighbor, the average energy of these barriers is then the activation energy for the diffusion of atomic hydrogens, regardless of the dimensionality of the space.

F. Power-law annealing behavior at long time

As reported in Ref. 14 and in this paper (see Sect. IV A), the long-time annealing behavior of atomic hydrogen tends towards $t^{-0.65}$. Twice this fractional power is the spectral dimension of the matrix upon which the species is diffusing, i.e., $d_s=1.3$, which is identical to the spectral dimension reported by Pfeffer[33] for the diffusion of molecular oxygen in silica. These results again support our proposal that diffusion in structural channels

(medium-range order of silica) is the root of the fractal kinetics. Since it is anticipated that in bulk oxide these structural channels are randomly oriented, it may be required that atomic hydrogen transport from one structural channel to another to complete its recombination reactions. The diffusion (or percolation) of atomic hydrogen from one channel to another is mathematically equivalent to their motion in a "percolation cluster." And it is known[34] that the spectral dimension for a percolation cluster embedded in any Euclidean space of dimension ≥ 2 is about $\frac{4}{3}=1.3$, which is identical to the spectral dimension observed here and reported in Refs. 14 and 33.

The apparent third-order kinetics for the production of interface defects through reaction with radiolytic hydrogen in SiO_2 thin-film–on–Si devices[35] as interpreted in Ref. 13 can also be understood in this picture: The *quasiepitaxy* effect can order these structural channels[11] during growth of thin oxide films on Si crystals, resulting in an effective dimension of 1. Third-order reaction kinetics is expected for a diffusion-controlled reaction in one-dimensional channels.[12]

V. SUMMARY

Long-time slow thermal annealing of radiolytic atomic hydrogen in amorphous silica studied by ESR was found to obey a t^{-f} law with a fractional power of $f \approx 0.65$. We argue that this outcome is due to the diffusion-limited dimerization of atomic hydrogen in structural channels (medium-range order) in the silica network. Short-time fast annealing is due to those hydrogen atoms that react with their immediate neighbors according to classical kinetics. These short-time, classical kinetic reactions primarily involve unlike reactants (e.g., dissolved CO molecules). The fraction of atomic hydrogen atoms undergoing classical kinetics was found to increase with increasing temperature.

Slower annealing kinetics of atomic hydrogens induced by 100-keV x rays in Suprasil 1 *vis-à-vis* in Suprasil 2 can be explained by the increase in the degree of medium-range order after the high-temperature thermal treatments which distinguish Suprasil 1 from Suprasil 2.

The observed fractional exponent of 0.65 can be understood as the diffusion of atomic hydrogens in a "percolation cluster" of these structural channels with spectral dimension of 1.3.

The effect of radiation type and dose on the decay kinetics of atomic hydrogen in silica is a decrease in the preexponential factors for H^0 diffusion with increasing energy deposition, with insignificant change in their activation energies.

---

*Present address: GEO Centers, Inc., Fort Washington, MD 20744.

[1]F. L. Galeener, Diffusion Defect Data **53-54**, 305 (1987); in *The Physics and Technology of Amorphous SiO_2,* edited by R. A. B. Devine (Plenum, New York, 1988), p. 1.

[2]S. Susman, D. L. Price, K. J. Volin, R. J. Dejus, and D. G. Montague, J. Non-Cryst. Solids **106**, 26 (1988).

[3]T. Egami, J. Non-Cryst. Solids **106**, 207 (1988).

[4]P. Vashishta, R. K. Kalia, and I. Ebbsjo, J. Non-Cryst. Solids **106**, 301 (1988).

[5]L. Cervinka, J. Non-Cryst. Solids **106**, 291 (1988).

[6]P. Brückner, J. Non-Cryst. Solids **5**, 123 (1970).

[7]J. H. Konnert, G. A. Ferguson, and J. Karle, Science **179**, 177 (1974).

[8]F. L. Galeener and A. C. Wright, Solid State Commun. **57**, 3841 (1986).

[9]F. J. Grunthaner, P. J. Grunthaner, R. P. Vasquez, B. F. Lewis, J. Masserjian, and A. Madhukar, Phys. Rev. Lett. **43**, 48 (1984).

[10]B. Agius, S. Rigo, F. Roche, M. Froment, C. Maillot, H. Roulet, and G. Dutour, Appl. Phys. Lett. **43**, 1683 (1979).

[11]A. G. Revesz, B. J. Mrstik, and H. L. Hughes, in *The Physics and Technology of Amorphous SiO_2,* edited by R. A. B. Devine (Plenum, New York, 1988), p. 297.

[12]R. Kopelman, Science **241**, 1620 (1988), and references therein.

[13]D. L. Griscom, J. Appl. Phys. **58**, 2524 (1985).

[14]T. E. Tsai and D. L. Griscom, J. Non-Cryst. Solids **106**, 374 (1988).

[15]A. Blumen, J. Klafter, and G. Zumofen, in *Optical Spectroscopy of Glasses,* edited by I. Zschokke (Reidel, Dordrecht, 1986), p. 199.

[16]K. Binder and A. P. Young, Rev. Mod. Phys. **58**, 801 (1986).

[17]*Relaxation in Complex Systems,* edited by K. L. Ngai and G. B. Wright (National Technical Information Service, Springfield, VA, 1984).

[18]*Transport and Relaxation in Random Materials,* edited by J. Klafter, R. J. Rubin, and M. F. Shlesinger (World Scientific, Philadelphia, 1985).

[19]S. Dattaguta, *Relaxation Phenomena in Condensed Matter Physics* (Academic, New York, 1987).

[20]A. K. Jonscher, *Dielectric Relaxation in Solids* (Chelsea Dielectrics, London, 1983).

[21]D. L. Griscom, J. Non-Cryst. Solids **68**, 301 (1984).

[22]D. L. Griscom, M. Stapelbroek, and E. J. Friebele, J. Chem. Phys. **78**, 1638 (1983).

[23]Since the apparent peak in f at about 105 K in Fig. 1(a) was interpreted as an artifact due to the side reactions discussed in the text, we then chose the lowest possible value of f in Eq. (7), which includes these side reactions, to achieve the fits represented in Fig. 1(b).

[24]In the kinetic fits of Figs. 2 and 3, there are five parameters to be determined. Among these, W (the fraction of total hydrogen which obeys classical kinetics) is determined uniquely by the fraction of atomic hydrogen remaining when the fractal kinetics dominates at long times. The parameters $k_a[A]$ and $k_b[\mathrm{H}]_0$ of the classical and the fractal kinetics were estimated by varying these quantities a decade at a time until a good fit was reached. The procedure was rather insensitive to $k_b[\mathrm{H}]_0$ in the case of classical kinetics; however, in the case of fractal kinetics the temperature dependence of $k_b[\mathrm{H}]_0$ was easily derived from the fitting procedure (see Table I).

[25]*Handbook of Chemistry and Physics,* 46th ed., edited by R. C. Weast (Chemical Rubber Co., Cleveland, 1965).

[26]T. E. Tsai, P. K. Tseng, and S. F. Tsai, J. Non-Cryst. Solids **81**, 147 (1986); T. E. Tsai, Chin. J. Phys. **23**, 293 (1986).
[27]G. Brauer and G. Boden, Diffusion Defect Data **53-54**, 173 (1987).
[28]L. P. Boesch and C. T. Moynihan, J. Non-Cryst. Solids **17**, 44 (1975).
[29]J. Kroh and A. Plonka, J. Phys. Chem. **79**, 2600 (1975).
[30]E. D. Sprague and D. Schulte-Frohlinde, J. Phys. Chem. **77**, 1222 (1973).
[31]S. Fujita, Phys. Status Solidi B **143**, 443 (1987).
[32]W. B. Jackson and J. Kakalios, Phys. Rev. B **37**, 1020 (1988).
[33]R. L. Pfeffer, in *The Physics and Chemistry of SiO_2 and the Si-SiO_2 Interface,* edited by C. R. Helms and B. E. Deal (Plenum, New York, 1988), p. 169.
[34]S. Alexander and R. Orbach, J. Phys. (Paris) Lett. **43**, L625 (1982).
[35]J. M. McGarrity, P. S. Winokur, H. E. Boesch, Jr., and F. B. McLean, in *The Physics of SiO_2 and Its Interfaces,* edited by S. T. Pantelides (Pergamon, New York, 1978), p. 428.